Anionic exopolysaccharide from *Cryptococcus laurentii* 70766 as an alternative for alginate for biomedical hydrogels

Masoud Hamidi[1,2Ω], Hafez Jafari[1Ω], Julia Siminska-Stanny[1], Oseweuba Valentine Okoro[1], Ahmed Fatimi[3], Amin Shavandi[1*]

[1] Université libre de Bruxelles (ULB), École polytechnique de Bruxelles – 3BIO-BioMatter, Avenue F.D. Roosevelt, 50 - CP 165/61, 1050 Brussels, Belgium Amin.Shavandi@ulb.be

[2] Department of Medical Biotechnology, Faculty of Paramedicine, Guilan University of Medical Sciences, Rasht, Iran

[3] Department of Chemistry, Polydisciplinary Faculty, Sultan Moulay Slimane University, P.O.BOX 592 Mghila, Beni-Mellal 23000, Morocco

Ω : These authors contributed equally to this work.

Abstract

Alginates are widely used polysaccharides for biomaterials engineering, which functional properties depend on guluronic and mannuronic acid as the building blocks. In this study, enzymatically crosslinked hydrogels based on sodium alginate (Na-Alg) and the exopolysaccharide (EPS) derived from *Cryptococcus laurentii* 70766 with glucuronic acid residues were synthesized and characterized as a new potential source of polysaccharide for biomaterials engineering. The EPS was extracted (1.05 ± 0.57 g/L) through ethanol precipitation. Then the EPS and Na-Alg were functionalized with tyramine hydrochloride to produce enzymatically crosslinked hydrogels in the presence of horseradish peroxidase (HRP) and H_2O_2. Major characteristics of the hydrogels such as gelling time, swelling ratio, rheology, cell viability, and biodegradability were studied. The swelling ratio and degradation profile of both hydrogels showed negative values, indicating an increased crosslinking degree and a lower water uptake percentage. The EPS hydrogel showed similar gelation kinetics compared to the Alg hydrogel. The EPS and its hydrogel were found cytocompatible. The results indicate the potential of EPS from *C. laurentii* 70766 for biomedical engineering due to its biocompatibility and degradability. Further studies are needed to confirm this EPS as an alternative for Alg in tissue engineering applications, particularly in the development of wound dressing products.

Keywords: exopolysaccharide; enzymatic crosslinking; hydrogel; *Cryptococcus laurentii*.

1. Introduction

Hydrogels are materials of unique characteristics capable of mimicking the hydration conditions of tissues and extracellular matrix, making them attractive for aiding the repair and regeneration of soft tissue [1]. As an FDA-approved biopolymer, alginate (Alg) has been studied to develop hydrogels for diverse applications such as tissue engineering (TE), drug delivery, and wound dressings due to their beneficial properties, e.g., biocompatibility, non-toxicity, high absorption capacity etc [2-4]. Alg is an anionic linear heteropolysaccharide that is characterized by repetitive units of 1,4-linked -D-mannuronic acid (M) and -L-guluronic acid (G) that are displayed as homosequences chain of MMMMM and GGGGG, interspersed with heterosequences of MGMGMG [5]. Alg may have higher G or higher M contents, witch Alg with a high G content capable of producing stiffer, brittle, and porous gels with greater strength, while Alg with a high M content produce more elastic and weaker gels [6]. Several studies have been published on Na-Alg-based hydrogels. Kaltostat™ and Tegagen™ are commercially available Alg dressings that contain only Na-Alg [7]. Despite the unique properties of Alg hydrogels that make them useful as wound dressings, they have some drawbacks, such as poor mechanical stability when swollen and hygroscopic property, leading to the need for a secondary dressing [7, 8]. During cross-linking with cations, cations diffuse from higher concentration locations to inner concentration regions, resulting in a nonuniform distribution of Alg in the gel matrix network [9]. Thus, Alg hydrogels are made using a combination of synthetic and natural polymers to overcome their poor mechanical stability, resulting in hydrogels with good mechanical properties [7].

Microbial exopolysaccharides (EPSs) have received a lot of attention recently in the search for novel biomaterials for TE and wound dressing engineering [10]. Microbial EPSs such as bacterial Alg, fungal chitosan, pullulan, scleroglucan, xanthan gum, bacterial cellulose, etc., are natural extracellular metabolites produced and secreted mainly by bacteria and fungi [11-14]. EPSs can be divided into homopolysaccharides (comprised of repeating units of monosaccharides like glucose, mannose, etc.) and heteropolysaccharides (containing three or more monosaccharides, e.g., arabinose, mannose, N-acetyl galactosamine, glucuronides and different derivatives of these subunits having phosphates, glycerol, or acetyl groups) [15-17].

The promising applications of EPSs in TE, food, cosmetics, and pharmaceuticals are due to their unique and complex chemical structures that offer beneficial bioactive functions such as biocompatibility, biodegradability, etc. [11, 17]. The monosaccharide units in EPSs have active hydroxyl, carboxyl, and amino groups, allowing for derivatization reactions, thus enhancing the possibility of novel crosslinking routines for hydrogel production while also endowing unique qualities for organism interaction [18]. Unlike other natural

polysaccharides extracted from other sources e.g., animals (chitin, chitosan, and hyaluronic acid), plants (starch, cellulose, glucomannan and pectin) and algae (agar, alginates and carrageenans), microbial EPSs production is season independent. For example, a physically crosslinked microbial EPS hydrogel from *Pseudomonas stutzeri* AS22, exhibited an *in vitro* and *in vivo* wound healing acceleration owing to its unique properties such as high antioxidant, anti-inflammatory activity, water uptake, as well as good mechanical stability [19]. Besides, a recent study reported the wound healing potential of EPS-based hydrogel produced by *Nostoc* spp. with iron ion resulting in the proliferation, and migration fibroblast cells, and enhanced wound healing [20]. In addition, the ability to use genetically engineered microbes under regulated fermentation settings could lead to the development of new EPSs with superior characteristics, opening up new areas of industrial application and increasing demand [19].

Because of the high yields of EPS biosynthesis and the ease with which yeast EPSs can be separated from growth media, researchers believe yeast EPSs should be prioritized over bacterial EPSs. Aside from that, yeast EPSs have gotten a lot of attention due to their intriguing biological activity, food, medicinal, and cosmetics applications [21]. *Cryptococcus laurentii* is a non-neoformans uncommon human pathogen (a saprophyte of pores and skin and seldom concerned in pulmonary and cutaneous contamination in humans) [21-23]. The microorganism produces EPSs of heterogeneous composition [24]. Growth conditions are known to affect the production and composition of the EPSs produced by different *C. laurentii* strains [25]. For example, Smirnou et al. achieved 4.3 g/L of EPS during 144 h by *C. laurentii* DSMZ 70766 in a simple batch cultivation (containing sucrose, yeast extract, $Na_2HPO_4 \times 12\ H_2O$, and $MgSO_4 \times 7\ H_2O$) [24]. Also, *C. laurentii* AL62 produced more than 5 g/l EPS in a medium containing sucrose at a concentration of 4% [26].

The strain employed in this study (*C. laurentii* 70766) was isolated from Californian almonds and classified in biosafety level 1 (based on the data sheet from DSMZ (German Collection of Microorganisms and Cell Cultures)). The EPS that was obtained from *C. laurentii* 70766 [24], is an acidic heteropolysaccharide glucuronoxylomannan composed of an α-(1-3)-linked mannan backbone, with O-6 and O-2 side chains of D-xylose and D-glucuronic acid residues [24]. The EPS from *C. laurentii* 70766, like other microbial EPSs, can be produced in bioreactors and is recovered using an environmentally friendly process that avoids the use of mineral acids or bases, which are employed when Alg is extracted. The use of these mineral acids and bases diminishes Alg quality via promoting its partial depolymerization [27]. This EPS is characterized by side branches of glucuronic acid residues [24] that are hypothesized to improve its gelation and viscoelastic properties [28]. Most importantly, the presence of the side branches may also enhance the ease of undertaking structural modifications,

thus reinforcing its suitability as a viable biomaterial for hydrogel formation. In the study by Smirnou et al., the EPS from *C. laurentii* 70766 was extracted, characterized, and its production optimized regarding pH, temperature, and aeration of the culture media, resulting in an efficient EPS production yield (4.3 g/L) [24]. Such a high yield is hypothesized to translate to a reduced unit production cost of the EPS for improved economic performance. Also, the EPS improved excisional wound healing in healthy rats and suggested that it may be a suitable material for biomaterials engineering [24].

In the present study enzymatic crosslinking has been proposed since it employs mild physiological conditions suitable for making hydrogels from natural polymers, thus avoiding the risk of losing their bioactivity in a strong chemical environment [29]. Enzymatic crosslinking is also preferred when the hydrogel is to be employed in enclosing biomolecules and living cells while also promoting high site-specificity and diminishing the potential for the formation of harmful by-products [30-32]. In addition to horseradish peroxidase (HRP), other enzymes such as transglutaminase and tyrosinase have also been employed in the production of hydrogelation. However, HRP has a number of advantages over these enzymes, such as faster hydrogelation time and the ability to fine-tune the hydrogelation rate and crosslinking density [33, 34]. Therefore, in the current study, our main objective was to analyze and compare the physicochemical and biological properties of the hydrogels synthesized via the enzymatic crosslinking of EPS produced from *C. laurentii* 70766 and Na-Alg in the presence of HRP and hydrogen peroxide (H_2O_2).

2. Materials and methods

2.1 Materials and reagents

Potato dextrose broth (PDB) was purchased from HiMedia, India (Model Number: M403-100G). Agar (CAS number: 9002-18-0) was obtained from AppliChem, Germany. Sucrose (CAS number: 57-50-1) was purchased from Fisher Chemical, Belgium. Magnesium sulfate heptahydrate (CAS number: 10034-99-8) and yeast extract (CAS number: 8013-01-2) were bought from Merck, Germany. Ethanol (96%) (CAS number: 64-17-5) was obtained from Avantor®, Belgium. Sodium alginate (Na-Alg) (W201502, alginic acid sodium salt from brown algae) having molecular weight (*Mw*) of 120-190 kDa with a M/G ratio of 1.61 (CAS number: 9005-38-3), 4-Morpholineethanesulfonic acid, 2-(N-Morpholino) ethanesulfonic acid (MES) (CAS number: 4432-31-9); 1-Ethyl-3-(3-dimethylaminopropyl) carbodiimide (EDC) (CAS number: 1892-57-5); N-ydroxysuccinimide (NHS), (CAS number: 6066-82-6), HRP (CAS number: 9003-99-0); and H_2O_2 (30%) (CAS number: 7722-84-1), were purchased from Merck (Darmstadt, Hessen, Germany). Tyramine hydrochloride CAS number: 60-19-

5) (HCl) was obtained from Carbosynth, UK. Dialysis membrane (*Mw* cut-off (MWCO): 14 kDa) was obtained from Membra-Cel™, USA.

2.2 Microorganism and culture condition

Cryptococcus laurentii 70766 was obtained from the German Collection of Microorganisms and Cell Cultures GmbH (DSMZ), Braunschweig, Germany and later was cultured on the potato dextrose agar (PDA) medium at 25℃. One fresh-single colony was used to inoculate 10 ml of the basal medium [24] for the inoculum preparation: Sucrose 35 g/L; yeast extract 3 g/L; $MgSO_4.7H_2O$ 0.5 g/L; $Na_2HPO_4.12H_2O$ 2.5 g/L; pH 6. After that, Erlenmeyer flasks (250 mL) cultures containing 100 mL medium were used for EPS production (144 h at 150 rpm and 25℃) in a shaking incubator (New Brunswick Classic C24 Incubator Shaker, USA) [24].

2.3 EPS extraction and purification

After incubation, the EPS supernatant was recovered by centrifugation at 8500 rpm for 30 minutes at 4℃ (3K3 centrifuge, Sigma Laboraxentrifugen, Germany). The EPS was precipitated from the supernatant by dropwise addition of cold ethanol while stirring; followed by keeping the precipitated EPS at 4℃ for 12 hours. The precipitated EPS was washed two times with ethanol and centrifuged at 8500 rpm for 20 minutes at 4℃ to obtain EPS pellets [35, 36]. The EPS pellets were dried at room temperature to a consistent mass, and finally, the pellets were dissolved in distilled water and lyophilized (Christ freeze-dryer alpha I-5). The EPS yield was reported as g of EPS per liter of culture media. The phenol-sulfuric acid method was used to determine the total carbohydrate content of the EPS, with glucose as the standard [37]. The average *Mw* of the EPS was 1×10^6 Da [24].

2.4 Fourier transform infrared (FT-IR) spectroscopy

FT-IR measurements were carried out at room temperature using a Jasco model FT/IR-6600 spectrometer using Spectra ManagerTM II Software. FT-IR spectra of the EPS and Na-Alg were obtained at a wavelength region of 4000 to 400 cm^{-1} [12].

2.5 Tyramine conjugation

EPS and Na-Alg were dissolved in MES buffer (1% w/v), and EDC (0.5% w/v) and NHS (0.3% w/v) were added to each solution to activate the carboxylic acid groups of EPS and Na-Alg for 30 minutes under stirring [38, 39]. Tyramine HCl (0.35 g/10 ml of MES buffer) was added dropwise to the solutions. The pH of the solutions was then maintained at 6 by dropwise adding 1 M HCl and allowing it to react with tyramine HCl at room temperature for 24 hours with stirring [38]. The resultant solutions were dialyzed for three days against deionized water in dialysis bags (cutoff: 14 kDa), and the water was changed every eight hours. Conjugated EPS (EPS-Ty)

and Alg-Ty were freeze-dried for further use. The UV–VIS spectra of unmodified/modified samples were obtained in the range of 220 to 400 nm to evaluate the extent of phenol group modification of the EPS and Alg. The calibration curve was plotted from known percentages of tyramine HCl in distilled water [38].

2.6 Hydrogels Formation and gelation times

Both HRP solution (1 U/mL) and H_2O_2 solution (1 mM) were prepared in distilled water. EPS-Ty and Alg-Ty solutions of 1% (w/v) were used for the hydrogel preparation. 180 µL of the EPS-Ty or Alg-Ty solutions were mixed with 10 µL of HRP and 10 µL of H_2O_2. The vial inversion test was performed at room temperature to obtain the gelation time [40]. The vials were monitored by inverting test tubes every five seconds after mixing EPS-Ty and Alg-Ty with HRP and H_2O_2. The gelation time was calculated as when there was no flow in the vial. Also, gelation time was estimated by rheology experiments (section 2.9).

2.7 Swelling and degradation of the hydrogels

The hydrogels (400 µL) were formed in the vials and accurately weighed (W_0). The hydrogel samples were subsequently incubated in 10 mL of PBS (pH 7.4) at 37℃. After 24 hours, the buffer solution was removed from the samples, placed in filter paper to remove excess liquid and the weight of the hydrogels was determined (W_t) to calculate the swelling ratio. The swelling ratio percentage was calculated using Equation (1) [41, 42]:

$$Swelling\ ratio\ (\%) = \frac{W_t}{W_0} * 100 \qquad \text{Equation (1)}$$

The degradation rate of hydrogels was investigated by the gravimetric method during incubation in PBS (pH 7.4) at 37 °C. After weighing the hydrogels every 24h, fresh PBS solutions were added to the hydrogels. The experiments were performed in triplicate [43].

2.8 Scanning electron microscopy

The morphology of the hydrogels was determined by the scanning electron microscope (SEM) (SU-70 Hitachi Ltd., Tokyo, Japan), operating at an accelerated voltage of 15 kV. The hydrogels in the volume of 900 µL were prepared and subsequently lyophilized. Before the experiment, the lyophilized hydrogels were cross-sectioned and gold-coated.

2.9 Rheological properties

The rheological measurements of EPS-Ty and Alg-Ty hydrogels were performed using an Anton Paar MRC 302 rheometer (Graz, Austria) equipped with a plate–plate geometry (25 mm). *In situ*, a volume of 300 µL of hydrogel was placed on the rheometer plate at 37℃. Oscillatory tests were used to determine the storage (G') and loss (G") moduli under the linear viscoelastic range (LVR). Amplitude sweep was performed from 1 to 1000%

at a constant frequency of 1 Hz, frequency sweep test was carried out at a constant strain of 0.1% over a frequency range of 0.1 to 50 Hz. Moreover, to study the gelation kinetics, the viscoelastic properties of hydrogel samples were determined using a time sweep oscillatory test at a constant frequency of 1 Hz and a strain of 0.1% under LVR at 37℃.

2.10 Effect of the unmodified EPS on the viability of human fibroblasts and macrophage cell lines

The effects of the different concentrations of the unmodified EPS (250, 500, 750, 1000, and 2000 µg/mL) on the viability of human macrophage (U937, ATCC: CRL-1593.2) and fibroblast (ATCC: CCL-186) cell lines were determined using a luminescence test based on Adenosine triphosphate quantification (CellTiter-Glo (Promega, Madison, Wisconsin)). Passage 19 cell lines (human macrophages and fibroblasts) were cultured in Roswell Park Memorial Institute Medium (RPMI-1640) and Dulbecco's modified Eagle's medium (DMEM) (LONZA, Verviers, Belgium), respectively supplemented with Fetal Calf Serum (FCS) (10% v/v), 1%(w/v) Penicillin-streptomycin (Gibco, Rockville, MD, USA) and incubated at 37℃ in a 5% CO_2. The cells were plated in triplicate in a white assay 96-well plate with a 10^4cells/well density [44]. 50 µL of EPS samples (dissolved in cell culture media) and 50 µL of RealTime-GloTM MT Cell Viability kit components were used to treat human fibroblast and macrophage cells. Control cells were grown in a medium that did not contain EPS. The viability of the cells was then determined by monitoring luminescence on a microplate luminometer (Centro XS LB 960-Berthold) at 0, 24 and 30 h, as proposed in the manufacturer's instructions.

2.11 3D cell encapsulation and hydrogel cytocompatibility tests

The cytocompatibility of hydrogels was evaluated through live/dead assay using 3T3 L fibroblast cell line and 3-(4,5-dimethylthiazol-2-yl)-5(3-carboxymethonyphenol)-2-(4-sulfophenyl)-2H-tetrazolium (MTS), [45]. First, the 3T3 L fibroblast cells were seeded on the hydrogel at a cell density of 10^4 cells/well in a 96-well plate for 3 days at 37℃ and the cell culture media was renewed every day. After 1, 2 and 3 days of culture, the 20 µL of MTS solution was added to the wells and incubated for 4 hours. Cell viability was determined by measuring the absorbance of the control (cell culture media) and samples at 490 nm using a microplate reader. Moreover, after 3 days of culture, the cell viability was evaluated by live/dead staining (ab115347, Abcam, UK) according to the manufacturer’s protocol. The cell-seeded hydrogels were stained with the live/dead reagent and incubated for 10 min at 37℃, after which the cells were investigated under a fluorescent microscope.

For the 3D cell encapsulation, the hydrogel precursors (1%) were dissolved in PBS solution and sterilized using syringe filters with sterile 0.22 µm pore size membranes. The hydrogel precursor (50 µL) containing HRP and cells with a final cell density of 5×10^5 cells/mL were mixed with the hydrogel precursors containing 1 mM

of H_2O_2 in a 96-well plate. After 10 min of incubation, the cell encapsulated hydrogels were cultured with 1 mL DMEM supplemented with 10% fetal calf serum (FCS), 200 U/mL penicillin, and 200 U/mL streptomycin. Cell viability was investigated after 3 days of incubation using Hoechst/ethidium homodimer I (EH1) staining. The cells were analyzed using a fluorescent microscope.

2.12 Statistical analysis

The statistical analyses were performed using three independent samples. The results were reported as mean ± standard error of the means. Data were analyzed as repeated measurement analysis of variance (ANOVA) to investigate the effects of the time, the concentrations of EPS and type of hydrogel on the cell viability and proliferation. Significant differences between means and multiple comparisons between means were analyzed by Tukey's test using Minitab 19 Statistical Software (Minitab®, PA, United States). Origin 2019b software (USA) and GraphPad Prism 9.0.0 (GraphPad Software, LLC, USA) were used for graphs.

3. Results and discussion

3.1 The EPS extraction, purification, and characterization

The total yield of the EPS produced by the *C. laurentii* strain was 1.05 ± 0.57 g/L and was determined to be mainly composed of carbohydrates (71.58 ± 1.43%, weight basis), using the phenol-sulfuric acid method. The residual portion of the EPS (28.42 ± 1.17%, weight basis) was attributed to ash and non-carbohydrate substituents in the EPS such as sulfate, pyruvate, methyl, or acetyl groups [46-48]. Notably, the yield 1.05 g/L reported in the current study was different from the EPS yield of about 1.8-2 g/L reported in the previous study [24] even though the same conditions were applied (temperature 25℃ and pH 6). In the study by Smirnou et al. [24], maximum EPS formation (4.3 g/L), occurred at the pH of 3, temperature 25℃, low aeration rates of 1 %<pO_2<10 % and after a 6-day incubation period in a bioreactor with 20-L working volume. Since the production of EPS from *C. laurentii* 70766 with the high content of glucuronic acid constituted a major objective of the study, pH 6 was applied to enhance the glucuronic acid content in EPS [24]. Furthermore, the present study did not seek to regulate the pO_2 in the shaking incubator. Such differences in pH values and lack of control over the aeriation rate for the EPS cultivation conditions may explain the differences in the EPS yields determined in the present study relative to the investigation undertaken by Smirnou et al. [24].

In comparison to Alg, which is usually extracted from brown algae under drastic conditions (acidic/basic extraction processes), leading to its partial depolymerization and increasing the cost of production [27, 49], the EPS from *C. laurentii* can be easily produced (extraction and purification) with eco-friendly processes, including

bioreactors. In addition, culture conditions such as carbon source, temperature, pH, aeration, and agitation can be controlled in terms of optimizing production.

FT-IR analysis was used to investigate the chemical structure of the extracted EPS and Na-Alg (Fig. 1). Regarding the EPS, the observed broad peak at 3225 cm^{-1} is related to the stretching vibrations of O–H [50] and the sharp peak observed at 2936 cm^{-1} is due to the stretching vibrations of C–H indicating the presence of the CH_3 functional group [51]. The peaks at 1566 cm^{-1} and 1418 cm^{-1} can be attributed to C=O stretching and C–H bending vibrations of carboxylic and CH_3 and/or CH_2 functional groups, respectively [50]. A sharp peak at 1032 cm^{-1} indicates the presence of C—O—C bonds [51]. Also, the Alg spectrum shows characteristic peaks around 1567 cm^{-1} and 1409 cm^{-1} corresponding to the asymmetric and symmetric stretching vibrations of the COO^- group on the polymeric backbone of Alg, respectively [52, 53]. The peak at 1024 cm^{-1} corresponds to the stretching vibration of the C-O bond [53]. The FT-IR analysis demonstrated a similarity in chemical bonds between EPS and Alg, particularly the presence of glucuronic units in the EPS structure.

3.2 Tyramine conjugation and hydrogel formation

The EPS and Alg were conjugated with tyramine using carbodiimide chemistry (Fig. 2b), and the conjugation of EPS-Ty and Alg-Ty was monitored by UV-vis analysis [54] (Fig. 2c). Compared to the unmodified EPS and Alg, the EPS-Ty and Alg-Ty conjugates showed UV absorbance at 275 nm corresponding to the absorbance of aromatic tyramine [55]. Moreover, the substitution degree of phenol groups was determined to be 0.417 ± 0.27 mmol/g and 0.428 ± 54 mmol/g of the EPS and Alg, respectively, using the tyramine HCl calibration curve.

HRP activated by H_2O_2 catalyzed the oxidation of the phenolic groups in the EPS and Alg chains, producing two phenoxy radicals in one catalytic cycle. The phenoxy radicals can react with each other in a radical coupling process, forming C-C and C-O bonds [56]. The carbon atom at the ortho position of phenyl groups and the phenolic oxygen formed a carbon-carbon bond or a carbon-oxygen linkage that connected the phenolic moieties at the ends of the polymers [57]. The gelation time obtained by vial inversion, was 99 ± 6s for the Alg-Ty hydrogel and 218 ± 6s for the EPS-Ty hydrogel, at the same concentration of polymers (1%), HRP (1 U/mL), and H_2O_2 (1mM).

Several studies used natural polysaccharide-phenol conjugate for enzymatic crosslinking and hydrogel formation in the presence of HRP and H_2O_2. Sakai et al. initially combined Alg with tyramine hydrochloride, then used HRP as a catalyst to prepare a Alg-Ty hydrogel. The results revealed that phenol crosslinking increased Alg's hydrophobicity, resulting in increased adsorption of cell-adhesive protein and the acquisition of cellular

adhesiveness in Alg [58]. Alg gels with crosslinks created by the HRP-catalyzed process were shown to be more stable than those with crosslinks formed by divalent ions alone [59]. Other biocompatible polymers such as dextran have been shown to be effective when phenol groups are included into them for HRP-catalyzed gelation [43, 60].

Moreover, Sakai et al. developed hydrogel constructs from polyglucuronic acid (PGU) - an bacterial EPS from *Sinorhizobium meliloti* M5N1CS that can be considered as an Alg alternative-[10, 27] by conjugating with tyramine through an HRP-catalyzed reaction and investigated the usefulness in TE field by using this derivative as a bioink component allowing gelation in extrusion-based 3D bioprinting [27]. Sakai et al. concluded that, like Alg, PGU may be effectively used and researched for new applications in TE, and that it might be used as a pectin and Alg substitute in the cosmetic and pharmaceutical industries [10].

Oliveira *et al.* developed three tyramine-substituted gellan gum (GG) hydrogels (with different amounts of HRP and H_2O_2 solutions). All three samples gelated in about 30 s [61]. GG is an anionic bacterial EPS and, like the EPS from *C. laurentii* has glucuronic acid in its structure (the repeating unit of GG consists of two D-glucose, one L-rhamnose and one D-glucuronic acid) [62], however unlike our EPS, the glucuronic acid units are in the polymer backbone. In another study, Tavakol *et al.* used repeated galacturonic acid methyl ester units in gum tragacanth (a heterogeneous highly branched anionic polysaccharide that galacturonic acid, xylose, fucose, arabinose, galactose, glucose, and traces of rhamnose are the primary components, with varying ratios in different species) [63] for the conjugation by tyramine and in situ forming hydrogel preparation via enzymatic crosslinking using HRP/H_2O_2 [64]. A fast gelation time (5–50 s) was achieved for the hydrogel suitable for drug delivery and TE applications [64]. The faster gelation time of hydrogels formed by GG (30 s) and gum tragacanth (5–50 s) in comparison to our study can be attributed to the increased number of phenolic groups per chain formed during tyramine conjugation with GG and gum tragacanth. Furthermore, Hasturk et al. reported that enzymatic crosslinking of silk fibroin in physiological buffers such as PBS or cell growth media was found to be much slower and produced mechanically weaker hydrogels than crosslinking in water [65]. It was suggested that these observations were likely due to the salting out effect of metal ions inducing self-assembly of hydrophobic domains containing many tyrosine groups required for enzymatic crosslinking [65].

There are also some reports in the literature regrading usage of microbial EPSs for hydrogel formation and other composites like electrospun nanofibers for wound healing applications. For instance, Ashraf et al. fabricated and characterized nanofiber skin substitutes composed of collagen/Na-Alg/polyethylene oxide/*Rhodotorula mucilaginosa* sp. GUMS16 produced EPS by means of the biaxial electrospinning method

[66]. They employed collagen from bovine tendon as a natural scaffold, Na-Alg as an absorber of excess wound fluids, and the EPS from GUMS16 strain as an antioxidant [66]. According to the findings, GUMS16-produced EPS in electrospun fibers might be considered a new biomacromolecule that increases cell survival and proliferation [66]. Also, Hivechi et al. used the EPS from GUMS16 strain as a bioactive agent in polycaprolactone (PCL) and gelatin nanofibers. In an animal model, they used nanofibers as a wound dressing material and assessed healing performance using macroscopic observation, wound closure computation, and microscopic assessment by histological analysis [67]. The wound closure percent increased from 72.33 ± 2.1% for PCL/Gelatin nanofiber to 99.81 ± 1.39% for PCL/Gelatin/EPS 2%, according to animal tests. Hivechi et al. therefore hypothesized that the antioxidant properties of the EPS was contributed to enhancing the healing process [67].

As a result, our findings show that enzymatic crosslinking is an effective method for rapidly forming hydrogels in situ, which are promising for use as injectable systems in biomedical applications such as TE and drug delivery.

3.3 Morphological structure, swelling and degradation properties of the hydrogels

The network microstructure of hydrogels is one of the essential features controlling protein adsorption, cell proliferation, mass transfer, and nutrition transfer [38, 68]. Furthermore, hydrogels containing interconnected porose networks can influence cell activity by promoting cell adhesion and cell-cell interaction [69]. As shown in Fig. 3a, there are no obvious differences in the morphology of the hydrogels [38]. The EPS-Ty and Alg-Ty hydrogels had a heterogeneous microstructure with irregular pore shapes randomly distributed throughout the hydrogels because of the polymers' structure and lyophilization process conditions (temperature and pressure), and the hydrogels' water content [70, 71]. This heterogeneous microstructure observation agrees with other studies. For example, Morshedloo *et al.* showed that peroxidase-mediated Alg-Ty hydrogel had an nonuniform porous morphology and noted that by the addition of gelatin, numerous homogeneous pores were created due to the reduction in mean pore size (MPS) and pore size polydispersity index (PSPI) [30]. Also, in the SEM images from the hydrogels produced by anionic EPSs from *Nostoc* sp. (strains PCC7936 and PCC7413), a fibrous-like porous network, as well as flaws and certain inhomogeneous structures in the form of continuous walls, were seen [20].

Fig. 3(c) shows the swelling ratio of EPS-Ty and Alg-Ty hydrogels after soaking the hydrogels up to 24 hours at 37℃. The swelling behavior of hydrogels is influenced by factors such as the degree of crosslinking, the possibility of ionic bonding with solvent (e.g., PBS solution), and the hydrophilicity of the hydrogel network [72]. The presence of cations in the immersing solution impacts the hydrogel behavior in swelling kinetics studies [72].

These cations, such as Ca^{2+} form ionic bonds, increase the degree of crosslinking, and decrease the water uptake percentage [72]. Thus, the interactions between the carboxylic group of the EPS, Alg and Ca^{2+} ions (might be present in the PBS), can reduce the number of hydrogen-binding donors and receptors available for water interaction, lowering the amount of water in the hydrogel network. The EPS-Ty and Alg-Ty hydrogels produced by enzymatic crosslinking, after immersion in PBS (ionic crosslinking) did not present any water absorption ability [73]. This observation agrees with the former investigations [61, 73]. For example, Oliveira et al. found that following immersion of the GG hydrogel in PBS (ionic crosslinking), the hydrogels (described in section 3.2), had no water absorption capabilities [61]. Similar results have been seen regarding the hydrogels produced by anionic EPSs from *Nostoc* sp. (strains PCC7936 and PCC7413). When hydrogels swelled for longer than 4 hours, the swelling degrees were decreased, due to the strong charge screening effect of trivalent ions (e.g., Fe^{3+} and Cr^{3+}) [20].

The degradation profile of hydrogels in this study was also determined by immersing the EPS-Ty and Alg-Ty hydrogels in PBS for 5 and 11 days at 37℃, respectively (Fig. 3b). The EPS-Ty hydrogel was comparatively more stable than the Alg-Ty hydrogel in PBS, partly due to the more crosslinking density.

The polydispersity index (*Mw*/*Mn*) of the EPS from *C. laurentii* 70766 is 1.352 [24], which is lower than the value of ~2, showing that some fractionation has occurred during the production process [74]. The *Mw* of the Na-Alg (W201502) used in this study is 120-190 kDa with a M/G ratio of 1.61 [75]. Furthermore, the M and G contents of Alg molecules extracted from various sources, as well as the length of each block, vary, and over 200 distinct Alg are currently produced. Commercially available Alg have a G-block content ranging from 14 to 31%. Only the G-blocks of Alg are thought to participate in the formation of hydrogels through intermolecular crosslinking with divalent cations (e.g., Ca^{2+}). The physical properties of Alg and its resulting hydrogels are thus influenced by the composition (i.e., M/G ratio), sequence, G-block length, and *Mw* [76-78]. As a result, the higher degree of crosslinking observed in the EPS-Ty hydrogel compared to Alg-Ty can be attributed to the EPS's higher glucuronic acid content (approximately 87% glucuronic acid in its structure [24]). Moreover, lower biodegradation profile of EPS-Ty hydrogel might be attributed to its lower swelling ratio probably due to its higher crosslinking density as well as its branching structure which hinders hydrolytic degradation compared to the Alg-Ty hydrogel [79, 80]. Further work will be undertaken in future studies to test this hypothesis.

3.4 Rheological properties of the hydrogels

The rheological properties of EPS-Ty and Alg-Ty hydrogels were examined by the oscillatory tests. First, the gelation kinetics of hydrogels was evaluated using an isothermal gelation test (supplementary Fig. 1

a&b). Based on time sweep results, both hydrogels showed an increase in the G' indicating the gelation process, and the G' reached 114 and 109 Pa after 2 min for Alg-Ty and EPS-Ty hydrogels, respectively. The G' of Alg-Ty reached a plateau after 3 min, however, the EPS-Ty hydrogel showed a continuous G' increment up to 10 min before reaching the plateau indicating slower gelation kinetic of EPS-Ty compared to Alg-Ty hydrogel. Hence, the final G' of the EPS-Ty hydrogel (362 Pa) was achieved after 10 min while, Alg-Ty hydrogel reached a G' of 140 Pa indicating higher stiffness of EPS-Ty hydrogel in comparison with Alg-Ty.

The storage modulus (G') and loss modulus (G") of EPS-Ty and Alg-Ty hydrogels were assessed by frequency sweep tests at a constant strain of 1% at 37℃ (supplementary Fig. 1 c&d). Both hydrogels exhibited a frequency-independent G' in the range of frequency of 1 to 10 Hz, and a higher value of G' compared to G", indicating the elastic and rigid structure of the hydrogels due to the presence of only covalent bonding [81-83]. The EPS-Ty hydrogel had a G' of 404 Pa, which was more than two times higher than the Alg-Ty hydrogel (140 Pa) (at 1 Hz). Moreover, the G" of the EPS-Ty hydrogel (56 Pa) was about 10 times higher compared to the Alg-Ty hydrogel (5 Pa). Given that both Alg-Ty and EPS-Ty showed a similar degree of phenol conjugation, this phenomenon could be attributed to EPS's high *Mw* (~1×10^6 Da [24]), and its branching structure (Fig. 2a) which endows the EPS with a higher viscosity than the Alg.

Moreover, an amplitude sweep test was performed to investigate the hydrogels' viscoelastic properties and critical strain (supplementary Fig. 1 e&f). This test was done on EPS-Ty and Alg-Ty hydrogels in the strain range from 0.1 to 1000 % at a constant frequency of 1 Hz and at 37℃. Alg-Ty hydrogel showed a strain independent G' up to 100 %, while EPS-Ty hydrogel LVR was up to 15 % (supplementary Fig. 1 e&f). Then, the hydrogels G' gradually decreased and crossed the G" attributed to a critical strain. The results showed that the critical strain of the Alg-Ty hydrogel (495 %) was higher than the EPS-Ty hydrogel (84%), indicating more stability of the Alg-Ty hydrogel against deformation and strain.

Furthermore, the dynamic viscosity assessment (supplementary Fig. 1 d) revealed a higher viscosity for EPS-Ty hydrogel precursor (6311.2 mPa·s) in comparison to the Alg-Ty hydrogel precursor (688.7 mPa·s) at a shear rate of 0.1 1/s. The higher viscosity of EPS-Ty precursor probably could be due to the branching structure of the EPS [24]. Besides, both Alg-Ty and EPS-Ty hydrogel precursors showed shear thinning behavior. The viscosity decreased to 5 mPa·s for both hydrogels by increasing the shear rate from 0.1 to 1000 1/s (supplementary Fig. 1 d).

Moreover, a recent study, reported an enzyme mediated crosslinking of EPS produced by *Sinorhizobium meliloti* for 3D bioprinting application [27]. The glucuronic based EPS gel precursor with 2 % concentration

showed a dynamic viscosity of around 1300 mPa·s at the shear rate of 0.1 1/s, while, the EPS presented in this study, exhibited higher dynamic viscosity at same shear rate with 1% concentration, indicating the potential of the EPS for 3D printing application. Our results showed superior rheological properties of EPS-Ty hydrogel compared to Alg-Ty hydrogel such as higher storage and loss modules, indicating that EPS presented in this study can be an alternative to the alginate to address its low mechanical stability.

3.5 Cell viability assay

Before investigating the cytocompatibility of the hydrogels, we determined the unmodified EPS cytocompatibility using fibroblast (ATCC: CCL-186) and human macrophage (U937, ATCC: CRL-1593.2) cell lines (Fig. 4 a&b). The EPS was cytocompatible at all concentrations (250-2000 µg/mL) for both cell lines. Furthermore, regarding the fibroblast cell line, the EPS promoted cell growth and proliferation of the cells (Fig a). These observations are consistent with other microbial EPSs cell toxicity results reported in the literature regarding human fibroblast cell lines. For example, the EPS (100 to 1000 µg/mL) from *R. mucilaginosa* sp. GUMS16 (a novel cold-adapted yeast), was biocompatible toward human dermal fibroblast (HDF) cell line during 48 h [35]. In addition, the EPS (10 to 1000 µg/mL) from *Weissella cibaria* EIR/P2 did not have a toxicity effect against human periodontal ligament fibroblast cells (hPDLFCs) during 24 hours and also showed proliferative effect on hPDLFCs [84]. Moreover, Liu et al. [85], Wang et al. [86], You et al. [87] and Uhliariková et al. [88], observed that the EPSs from *Phomopsis liquidambari* NJUSTb1 (between 31.25-500 µg/mL), *Lactobacillus plantarum* JLK0142 (between 50-1000 µg/mL), *Lactobacillus pentosus* LZ-R-17 (between 50-400 µg/mL) and the cyanobacterium *Nostoc* sp. (between 0–1000 µg/mL), had no toxicity effects on the macrophage cell line (RAW 264.7). Moreover, in another research, Alvarez et al. produced hydrogels from the EPSs produced by other strains of cyanobacterium *Nostoc* (*Nostoc* PCC 7413 and *Nostoc* PCC 7936) by gelation with $FeCl_3$. The results revealed enhanced biocompatibility and the ability for stimulating wound healing. Furthermore, EPS hydrogels aided fibroblast migration, which can be included in the evolution of the regeneration process [20].

As reported by Smirnou *et al.*, the EPS from *C. laurentii* 70766, employed in the current study showed a significant wound healing effect in healthy rats [24]. The proliferation of fibroblasts is an important step in wound healing [89]. The cell proliferative activities of some microbial EPSs are attributed to the presence of sulfate and carboxylate groups [90]. Based on the previous study [24], the EPS comprises more than 85% acidic glucuronoxylomannan (GXM). So, net anionic charges on the EPS may facilitate interactions with cationic amino acids on key effector protein molecules of cell proliferation, such as basic fibroblast growth factors, adhesion molecules, and cytokines [91-93]. Hence, the fibroblast cell proliferative activities of the EPS from *C. laurentii*

70766 confirmed in this study could be responsible for its improved *in vivo* wound healing effect that has been confirmed before by Smirnou et al. [24].

Then, we investigated the cytocompatibility of the EPS-Ty hydrogel and compared it with the Alg-Ty hydrogel toward 3T3 L fibroblast cell line using MTS and live/dead staining. The MTS results (Fig. 4c) showed that both Alg-Ty and EPS-Ty hydrogels were biocompatible, and the cells could grow on the hydrogels without any significant difference compared to the control (cell culture media) after 24 and 72 h.

Moreover, live/dead assay results (Fig. 4d) confirmed the biocompatibility of EPS-Ty and Alg-Ty hydrogels compared to the control (TCPS). Both hydrogels showed a higher number of live cells (green) than the dead cells (red) and well-distributed cells on the hydrogels, showing the non-toxicity of the hydrogels.

Additionally, the 3D cell encapsulation of fibroblast cells within the enzymatically crosslinked EPS-Ty and Alg-Ty hydrogels was assessed after 1 (Fig. 4e) and 3 days (Fig. 4f) using Hoechst/ethidium homodimer staining. Both cell-laden Alg-Ty and EPS-Ty hydrogels could support the proliferation of fibroblast cells after 3 days with a high percentage of viable cells compared to dead cells (red). Recent research suggests that enzyme-mediated hydrogels could be candidates for 3D cell encapsulation at low H_2O_2 concentration [94, 95].

4. Conclusions

In the present study, an anionic EPS produced by *C. laurentii* 70766 was conjugated with tyramine and enzymatically crosslinked employing HRP-mediated crosslinking to form a stable hydrogel, and the EPS based hydrogel was compared with alginate-tyramine hydrogel as a commercially available biopolymer The EPS hydrogel showed similar gelation kinetic, swelling ratio, rheological properties, as well as prolonged degradation profile compared to the alginate-based hydrogel. Moreover, The EPS demonstrated no adverse effect on the viability and proliferation of human macrophage and fibroblast cells indicating a potential for developing of wound dressing hydrogels. However, the low yield of EPS produced by *C. laurentii* 70766 (1.05 g/L) can hinder its large-scale production which must be enhanced by optimization of extraction parameters (i.e., temperature, pH etc.). Furthermore, there is a need to elucidate the regulatory mechanism of EPS induced wound healing since such knowledge will reveal the dynamics of EPS-enabled wound healing when subjected to various physical and biological conditions. Notably, despite the existing challenges, it is important to acknowledge that the present study highlights new knowledge regarding important biological properties of the novel anionic EPS produced by *C. laurentii* 70766 and thus reveals new pathways for future clinical studies with respect to their potential wound healing capacity in human subjects.

CRediT authorship contribution statement

Masoud Hamidi: Conceptualization, Methodology, Formal analysis, Investigation, Validation, Writing-original draft, Writing-review & editing. **Hafez Jafari:** Conceptualization, Methodology, Formal analysis, Investigation, Writing review & editing. **Julia Siminska-Stanny**: Investigation, Methodology, Writing-review & editing. **Oseweuba Valentine Okoro:** Investigation, Validation, Writing-original draft, Writing-review & editing. **Ahmed Fatimi:** Investigation, Validation, Writing-review & editing. **Amin Shavandi:** Conceptualization, Validation, Resources, Supervision, Writing review & editing, Visualization, Project administration, Funding acquisition.

Declaration of competing interest

The authors declare that they have no conflict of interest.

Acknowledgements

M.H. would like to acknowledge the postdoctoral fellowship provided by the European Program IF@ULB-MARIE SKŁODOWSKA-CURIE Cofund Action (European Horizon 2020). This project has received funding from the European Union's Horizon 2020 research and innovation program under the Marie Skłodowska-Curie grant agreement No. 801505. The graphical abstract and Fig. 1 were prepared using Biorender.com. Also, we must thank Dr. Mahta Mirzaei for her kind help in cell viability assays using RealTime-Glo™ MT Cell Viability kit.

References

[1] M. Beaumont, R. Tran, G. Vera, D. Niedrist, A. Rousset, R. Pierre, V.P. Shastri, A. Forget, Hydrogel-Forming Algae Polysaccharides: From Seaweed to Biomedical Applications, Biomacromolecules (2021).
[2] M.I. Neves, L. Moroni, C.C. Barrias, Modulating Alginate Hydrogels for Improved Biological Performance as Cellular 3D Microenvironments, 8 (2020).
[3] V.G. Muir, J.A. Burdick, Chemically Modified Biopolymers for the Formation of Biomedical Hydrogels, Chemical Reviews (2020).
[4] A. Shavandi, S. Hosseini, O.V. Okoro, L. Nie, F. Eghbali Babadi, F. Melchels, 3D Bioprinting of Lignocellulosic Biomaterials, Adv Healthc Mater 9(24) (2020) e2001472.
[5] I. Neamtu, A.P. Chiriac, L.E. Nita, A. Diaconu, A.G. Rusu, Chapter 11 - Nanogels Containing Polysaccharides for Bioapplications, in: C. Vasile (Ed.), Polymeric Nanomaterials in Nanotherapeutics, Elsevier2019, pp. 387-420.
[6] R. Gheorghita, L. Anchidin-Norocel, R. Filip, M. Dimian, M. Covasa, Applications of Biopolymers for Drugs and Probiotics Delivery, Polymers 13(16) (2021) 2729.
[7] B.A. Aderibigbe, B. Buyana, Alginate in wound dressings, Pharmaceutics 10(2) (2018) 42.
[8] R. Gheorghita Puscaselu, A. Lobiuc, M. Dimian, M. Covasa, Alginate: From food industry to biomedical applications and management of metabolic disorders, Polymers 12(10) (2020) 2417.
[9] S. Shen, X. Chen, Z. Shen, H. Chen, Marine polysaccharides for wound dressings application: An overview, Pharmaceutics 13(10) (2021) 1666.
[10] Z.E. Dibazar, M. Mohammadpour, H. Samadian, S. Zare, M. Azizi, M. Hamidi, R. Elboutachfaiti, E. Petit, C. Delattre, Bacterial Polyglucuronic Acid/Alginate/Carbon Nanofibers Hydrogel Nanocomposite as a Potential Scaffold for Bone Tissue Engineering, Materials 15(7) (2022) 2494.

[11] Y. Ju, K. Shan, W. Liu, C. Xi, Y. Zhang, W. Wang, C. Wang, R. Cao, W. Zhu, H. Wang, Y. Zhao, L. Hao, Effect of Different Initial Fermentation pH on Exopolysaccharides Produced by *Pseudoalteromonas agarivorans* Hao 2018 and Identification of Key Genes Involved in Exopolysaccharide Synthesis via Transcriptome Analysis, Mar. Drugs 20(2) (2022) 89.
[12] R. Mirzaei Seveiri, M. Hamidi, C. Delattre, H. Sedighian, G. Pierre, B. Rahmani, S. Darzi, C. Brasselet, F. Karimitabar, A. Razaghpoor, J. Amani, Characterization and Prospective Applications of the Exopolysaccharides Produced by *Rhodosporidium babjevae*, Adv Pharm Bull 10(2) (2020) 254-263.
[13] O.V. Okoro, A.R. Gholipour, F. Sedighi, A. Shavandi, M. Hamidi, Optimization of Exopolysaccharide (EPS) Production by *Rhodotorula mucilaginosa* sp. GUMS16, ChemEngineering 5(3) (2021) 39.
[14] M.L. Cázares-Vásquez, R. Rodríguez-Herrera, C.N. Aguilar-González, A. Sáenz-Galindo, J.F. Solanilla-Duque, J.C. Contreras-Esquivel, A.C. Flores-Gallegos, Microbial Exopolysaccharides in Traditional Mexican Fermented Beverages, Fermentation 7(4) (2021) 249.
[15] Y. Fan, X. Li, R. Tian, R. Tang, J. Zhang, Characterization and Biological Activity of a Novel Exopolysaccharide Produced by *Pediococcus pentosaceus* SSC-12 from Silage, Microorganisms 10(1) (2022) 18.
[16] P. Petrova, A. Arsov, I. Ivanov, L. Tsigoriyna, K. Petrov, New Exopolysaccharides Produced by *Bacillus licheniformis* 24 Display Substrate-Dependent Content and Antioxidant Activity, Microorganisms 9(10) (2021) 2127.
[17] Hamidi, O.V. Okoro, P.B. Milan, M.R. Khalili, H. Samadian, L. Nie, A. Shavandi, Fungal exopolysaccharides: Properties, sources, modifications, and biomedical applications, Carbohydr. Polym. (2022) 119152.
[18] Q. Yang, J. Peng, H. Xiao, X. Xu, Z. Qian, Polysaccharide hydrogels: Functionalization, construction and served as scaffold for tissue engineering, Carbohydr. Polym. (2021) 118952.
[19] H. Maalej, D. Moalla, C. Boisset, S. Bardaa, H.B. Ayed, Z. Sahnoun, T. Rebai, M. Nasri, N. Hmidet, Rhelogical, dermal wound healing and in vitro antioxidant properties of exopolysaccharide hydrogel from Pseudomonas stutzeri AS22, Colloids Surf. B. Biointerfaces 123 (2014) 814-824.
[20] X. Alvarez, A. Alves, M.P. Ribeiro, M. Lazzari, P. Coutinho, A. Otero, Biochemical characterization of *Nostoc* sp. exopolysaccharides and evaluation of potential use in wound healing, Carbohydr. Polym. 254 (2021) 117303.
[21] Y. Rahbar Saadat, A. Yari Khosroushahi, B. Pourghassem Gargari, Yeast exopolysaccharides and their physiological functions, Folia Microbiologica 66(2) (2021) 171-182.
[22] M. Gupta, A.K. Mishra, S.K. Singh, *Cryptococcus laurentii* fungemia in a low birth weight preterm neonate: India, Journal of infection and public health 11(6) (2018) 896-897.
[23] J.E. Bennett, R. Dolin, M.J. Blaser, Mandell, Douglas, and Bennett's Principles and Practice of Infectious Diseases E-Book, Elsevier Health Sciences2019.
[24] D. Smirnou, D. Hrubošová, J. Kulhánek, K. Švík, L. Bobková, V. Moravcová, M. Krčmář, L. Franke, V. Velebný, *Cryptococcus laurentii* extracellular biopolymer production for application in wound management, Applied biochemistry and biotechnology 174(4) (2014) 1344-1353.
[25] E. Breierová, Z. Hromádková, E. Stratilová, V. Sasinková, A. Ebringerová, Effect of salt stress on the production and properties of extracellular polysaccharides produced by *Cryptococcus laurentii*, Zeitschrift für Naturforschung C 60(5-6) (2005) 444-450.
[26] I. Gientka, S. Błażejak, L. Stasiak-Różańska, A. Chlebowska-Śmigiel, Exopolysaccharides from yeast: insight into optimal conditions for biosynthesis, chemical composition and functional properties? review, Acta Scientiarum Polonorum Technologia Alimentaria 14(4) (2015) 283-292.
[27] S. Sakai, T. Kotani, R. Harada, R. Goto, T. Morita, S. Bouissil, P. Dubessay, G. Pierre, P. Michaud, R. El Boutachfaiti, M. Nakahata, M. Kojima, E. Petit, C. Delattre, Development of phenol-grafted polyglucuronic acid and its application to extrusion-based bioprinting inks, Carbohydr. Polym. 277 (2022) 118820.
[28] D. Gawkowska, J. Cybulska, A. Zdunek, Structure-Related Gelling of Pectins and Linking with Other Natural Compounds: A Review, Polymers 10(7) (2018) 762.
[29] V.S. Ghorpade, Preparation of hydrogels based on natural polymers via chemical reaction and cross-Linking, Hydrogels Based on Natural Polymers, Elsevier2020, pp. 91-118.
[30] F. Morshedloo, A.B. Khoshfetrat, D. Kazemi, M. Ahmadian, Gelatin improves peroxidase-mediated alginate hydrogel characteristics as a potential injectable hydrogel for soft tissue engineering applications, Journal of Biomedical Materials Research Part B: Applied Biomaterials 108(7) (2020) 2950-2960.
[31] Y. Zhong, J. Wang, Z. Yuan, Y. Wang, Z. Xi, L. Li, Z. Liu, X. Guo, A mussel-inspired carboxymethyl cellulose hydrogel with enhanced adhesiveness through enzymatic crosslinking, Colloids Surf. B. Biointerfaces 179 (2019) 462-469.
[32] H. Jafari, C. Delporte, K.V. Bernaerts, H. Alimoradi, L. Nie, D. Podstawczyk, K.C. Tam, A. Shavandi, Synergistic complexation of phenol functionalized polymer induced in situ microfiber formation for 3D printing of marine-based hydrogels, Green Chemistry 24(6) (2022) 2409-2422.

[33] L. Wang, J. Li, D. Zhang, S. Ma, J. Zhang, F. Gao, F. Guan, M. Yao, Dual-enzymatically crosslinked and injectable hyaluronic acid hydrogels for potential application in tissue engineering, RSC Advances 10(5) (2020) 2870-2876.
[34] S. Liu, X. Zhou, L. Nie, Y. Wang, Z. Hu, O.V. Okoro, A. Shavandi, L. Fan, Anisotropic PLGA microsphere/PVA hydrogel composite with aligned macroporous structures for directed cell adhesion and proliferation, International Journal of Polymeric Materials and Polymeric Biomaterials (2021) 1-10.
[35] M. Hamidi, A.R. Gholipour, C. Delattre, F. Sesdighi, R. Mirzaei Seveiri, A. Pasdaran, S. Kheirandish, G. Pierre, P. Safarzadeh Kozani, P. Safarzadeh Kozani, F. Karimitabar, Production, characterization and biological activities of exopolysaccharides from a new cold-adapted yeast: *Rhodotorula mucilaginosa* sp. GUMS16, Int J Biol Macromol 151 (2020) 268-277.
[36] I.S. Choi, S.H. Ko, M.E. Lee, H.M. Kim, J.E. Yang, S.-G. Jeong, K.H. Lee, J.Y. Chang, J.-C. Kim, H.W. Park, Production, Characterization, and Antioxidant Activities of an Exopolysaccharide Extracted from Spent Media Wastewater after *Leuconostoc mesenteroides* WiKim32 Fermentation, ACS omega 6(12) (2021) 8171-8178.
[37] M. Dubois, K.A. Gilles, J.K. Hamilton, P.t. Rebers, F. Smith, Colorimetric method for determination of sugars and related substances, Anal. Chem. 28(3) (1956) 350-356.
[38] H. Jafari, A. Dadashzadeh, S. Moghassemi, P. Zahedi, C.A. Amorim, A. Shavandi, Ovarian Cell Encapsulation in an Enzymatically Crosslinked Silk-Based Hydrogel with Tunable Mechanical Properties, Gels 7(3) (2021) 138.
[39] D. Lee, J.P. Park, M.-Y. Koh, P. Kim, J. Lee, M. Shin, H. Lee, Chitosan-catechol: a writable bioink under serum culture media, Biomaterials Science 6(5) (2018) 1040-1047.
[40] R. Ziadlou, S. Rotman, A. Teuschl, E. Salzer, A. Barbero, I. Martin, M. Alini, D. Eglin, S. Grad, Optimization of hyaluronic acid-tyramine/silk-fibroin composite hydrogels for cartilage tissue engineering and delivery of anti-inflammatory and anabolic drugs, Materials Science and Engineering: C 120 (2021) 111701.
[41] A. Hajighasem, K. Kabiri, Cationic highly alcohol-swellable gels: synthesis and characterization, Journal of Polymer Research 20(8) (2013) 1-9.
[42] L. Ma, W. Su, Y. Ran, X. Ma, Z. Yi, G. Chen, X. Chen, Z. Deng, Q. Tong, X. Wang, Synthesis and characterization of injectable self-healing hydrogels based on oxidized alginate-hybrid-hydroxyapatite nanoparticles and carboxymethyl chitosan, International Journal of Biological Macromolecules 165 (2020) 1164-1174.
[43] R. Jin, C. Hiemstra, Z. Zhong, J. Feijen, Enzyme-mediated fast in situ formation of hydrogels from dextran–tyramine conjugates, Biomaterials 28(18) (2007) 2791-2800.
[44] I. Alimov, S. Menon, N. Cochran, R. Maher, Q. Wang, J. Alford, J.B. Concannon, Z. Yang, E. Harrington, L. Llamas, Bile acid analogues are activators of pyrin inflammasome, Journal of Biological Chemistry 294(10) (2019) 3359-3366.
[45] H. Jafari, C. Delporte, K.V. Bernaerts, H. Alimoradi, L. Nie, D.A. Podstawczyk, K.C. Tam, A. Shavandi, Synergistically complexation of phenol functionalized polymer induced in-situ microfiber formation for 3D printing of marine-based hydrogel, Green Chem. (2022).
[46] C. Delattre, G. Pierre, C. Laroche, P. Michaud, Production, extraction and characterization of microalgal and cyanobacterial exopolysaccharides, Biotechnology Advances 34(7) (2016) 1159-1179.
[47] K. Buksa, M. Kowalczyk, J. Boreczek, Extraction, purification and characterisation of exopolysaccharides produced by newly isolated lactic acid bacteria strains and the examination of their influence on resistant starch formation, Food Chem. 362 (2021) 130221.
[48] C.E. Escárcega-González, J.A. Garza-Cervantes, A. Vázquez-Rodríguez, J.R. Morones-Ramírez, Bacterial Exopolysaccharides as Reducing and/or Stabilizing Agents during Synthesis of Metal Nanoparticles with Biomedical Applications, International Journal of Polymer Science 2018 (2018) 7045852.
[49] R. Elboutachfaiti, C. Delattre, E. Petit, P. Michaud, Polyglucuronic acids: Structures, functions and degrading enzymes, Carbohydr. Polym. 84(1) (2011) 1-13.
[50] O.V. Okoro, Z. Sun, The characterisation of biochar and biocrude products of the hydrothermal liquefaction of raw digestate biomass, Biomass Conversion and Biorefinery (2020).
[51] D.S. Vasanthakumari, S. Harikumar, D.J. Beena, A. Pandey, K.M. Nampoothiri, Physicochemical characterization of an exopolysaccharide produced by a newly isolated *Weissella cibaria*, Applied biochemistry and biotechnology 176(2) (2015) 440-453.
[52] D. Komoto, T. Furuike, H. Tamura, Preparation of polyelectrolyte complex gel of sodium alginate with chitosan using basic solution of chitosan, International journal of biological macromolecules 126 (2019) 54-59.
[53] S. Sellimi, I. Younes, H.B. Ayed, H. Maalej, V. Montero, M. Rinaudo, M. Dahia, T. Mechichi, M. Hajji, M. Nasri, Structural, physicochemical and antioxidant properties of sodium alginate isolated from a Tunisian brown seaweed, International journal of biological macromolecules 72 (2015) 1358-1367.

[54] S. Saghati, A.B. Khoshfetrat, H. Tayefi Nasrabadi, L. Roshangar, R. Rahbarghazi, Fabrication of alginate-based hydrogel cross-linked via horseradish peroxidase for articular cartilage engineering, BMC Res. Notes 14(1) (2021) 384.
[55] D. Spasojevic, M. Prokopijevic, O. Prodanovic, N. Zelenovic, N. Polovic, K. Radotic, R. Prodanovic, Peroxidase-Sensitive Tyramine Carboxymethyl Xylan Hydrogels for Enzyme Encapsulation, Macromolecular Research 27(8) (2019) 764-771.
[56] S. Sakai, M. Nakahata, Horseradish Peroxidase Catalyzed Hydrogelation for Biomedical, Biopharmaceutical, and Biofabrication Applications, Chemistry – An Asian Journal 12(24) (2017) 3098-3109.
[57] S.V. Gohil, S.B. Brittain, H.-M. Kan, H. Drissi, D.W. Rowe, L.S. Nair, Evaluation of enzymatically crosslinked injectable glycol chitosan hydrogel, Journal of Materials Chemistry B 3(27) (2015) 5511-5522.
[58] S. Sakai, Y. Yamada, T. Zenke, K. Kawakami, Novel chitosan derivative soluble at neutral pH and in-situ gellable via peroxidase-catalyzed enzymatic reaction, J. Mater. Chem. 19(2) (2009) 230-235.
[59] S. Sakai, K. Hirose, K. Moriyama, K. Kawakami, Control of cellular adhesiveness in an alginate-based hydrogel by varying peroxidase and H2O2 concentrations during gelation, Acta Biomater. 6(4) (2010) 1446-1452.
[60] H. Zhang, J. Cheng, Q. Ao, Preparation of Alginate-Based Biomaterials and Their Applications in Biomedicine, Mar. Drugs 19(5) (2021) 264.
[61] I.M. Oliveira, C. Gonçalves, M.E. Shin, S. Lee, R.L. Reis, G. Khang, J.M. Oliveira, Enzymatically crosslinked tyramine-gellan gum hydrogels as drug delivery system for rheumatoid arthritis treatment, Drug Delivery and Translational Research 11(3) (2021) 1288-1300.
[62] K.K. Sadasivuni, K. Deshmukh, M.A. AlMaadeed, 3D and 4D Printing of Polymer Nanocomposite Materials: Processes, Applications, and Challenges, Elsevier2019.
[63] M. Nejatian, S. Abbasi, F. Azarikia, Gum Tragacanth: Structure, characteristics and applications in foods, International Journal of Biological Macromolecules 160 (2020) 846-860.
[64] M. Tavakol, E. Vasheghani-Farahani, M.A. Mohammadifar, M. Soleimani, S. Hashemi-Najafabadi, Synthesis and characterization of an in situ forming hydrogel using tyramine conjugated high methoxyl gum tragacanth, J. Biomater. Appl. 30(7) (2016) 1016-1025.
[65] O. Hasturk, K.E. Jordan, J. Choi, D.L. Kaplan, Enzymatically crosslinked silk and silk-gelatin hydrogels with tunable gelation kinetics, mechanical properties and bioactivity for cell culture and encapsulation, Biomaterials 232 (2020) 119720.
[66] S.S. Ashraf, K. Parivar, N.H. Roodbari, S. Mashayekhan, N. Amini, Fabrication and characterization of biaxially electrospun collagen/alginate nanofibers, improved with Rhodotorula mucilaginosa sp. GUMS16 produced exopolysaccharides for wound healing applications, International Journal of Biological Macromolecules 196 (2022) 194-203.
[67] A. Hivechi, P.B. Milan, K. Modabberi, M. Amoupour, K. Ebrahimzadeh, A.R. Gholipour, F. Sedighi, N. Amini, S.H. Bahrami, A. Rezapour, M. Hamidi, C. Delattre, Synthesis and Characterization of Exopolysaccharide Encapsulated PCL/Gelatin Skin Substitute for Full-Thickness Wound Regeneration, Polymers 13(6) (2021) 854.
[68] J. Yang, Y. Li, Y. Liu, D. Li, L. Zhang, Q. Wang, Y. Xiao, X. Zhang, Influence of hydrogel network microstructures on mesenchymal stem cell chondrogenesis in vitro and in vivo, Acta Biomater. 91 (2019) 159-172.
[69] B.-H. Lee, B. Li, S.A. Guelcher, Gel microstructure regulates proliferation and differentiation of MC3T3-E1 cells encapsulated in alginate beads, Acta Biomater. 8(5) (2012) 1693-1702.
[70] J. Yan, X. Jia, W. Yan, L. Yin, Double-Network Hydrogels of Corn Fiber Gum and Soy Protein Isolate: Effect of Biopolymer Constituents and pH Values on Textural Properties and Microstructures, Foods 10(2) (2021) 356.
[71] C. Chi, X. Li, Y. Zhang, S. Miao, L. Chen, L. Li, Y. Liang, Understanding the effect of freeze-drying on microstructures of starch hydrogels, Food Hydrocolloids 101 (2020) 105509.
[72] Y. Xu, Y. Li, Q. Chen, L. Fu, L. Tao, Y. Wei, Injectable and self-healing chitosan hydrogel based on imine bonds: design and therapeutic applications, Int. J. Mol. Sci. 19(8) (2018) 2198.
[73] Y. Huang, H. Yu, C. Xiao, pH-sensitive cationic guar gum/poly (acrylic acid) polyelectrolyte hydrogels: Swelling and in vitro drug release, Carbohydr. Polym. 69(4) (2007) 774-783.
[74] K.I. Draget, Alginates, Handbook of hydrocolloids, Elsevier2009, pp. 807-828.
[75] Z. Emami, M. Ehsani, M. Zandi, R. Foudazi, Controlling alginate oxidation conditions for making alginate-gelatin hydrogels, Carbohydr. Polym. 198 (2018) 509-517.
[76] K.Y. Lee, D.J. Mooney, Alginate: properties and biomedical applications, Prog. Polym. Sci. 37(1) (2012) 106-126.
[77] K. Draget, G.S. Bræk, O. Smidsrød, Alginic acid gels: the effect of alginate chemical composition and molecular weight, Carbohydr. Polym. 25(1) (1994) 31-38.
[78] D.C. Aduba, H. Yang, Polysaccharide Fabrication Platforms and Biocompatibility Assessment as Candidate Wound Dressing Materials, Bioengineering (Basel) 4(1) (2017).

[79] G. Hoti, F. Caldera, C. Cecone, A. Rubin Pedrazzo, A. Anceschi, S.L. Appleton, Y. Khazaei Monfared, F. Trotta, Effect of the cross-linking density on the swelling and rheological behavior of Ester-bridged β-cyclodextrin nanosponges, Materials 14(3) (2021) 478.
[80] M.B. Browning, S.N. Cereceres, P.T. Luong, E.M. Cosgriff-Hernandez, Determination of the in vivo degradation mechanism of PEGDA hydrogels, Journal of Biomedical Materials Research Part A 102(12) (2014) 4244-4251.
[81] F. Cuomo, M. Cofelice, F. Lopez, Rheological characterization of hydrogels from alginate-based nanodispersion, Polymers 11(2) (2019) 259.
[82] J. Hou, C. Li, Y. Guan, Y. Zhang, X. Zhu, Enzymatically crosslinked alginate hydrogels with improved adhesion properties, Polymer Chemistry 6(12) (2015) 2204-2213.
[83] S.A. Glukhova, V.S. Molchanov, B.V. Lokshin, A.V. Rogachev, A.A. Tsarenko, T.D. Patsaev, R.A. Kamyshinsky, O.E. Philippova, Printable Alginate Hydrogels with Embedded Network of Halloysite Nanotubes: Effect of Polymer Cross-Linking on Rheological Properties and Microstructure, Polymers (Basel) 13(23) (2021).
[84] H. Kibar, Y.E. Arslan, A. Ceylan, B. Karaca, O. Haliscelik, F. Kiran, *Weissella cibaria* EIR/P2-derived exopolysaccharide: A novel alternative to conventional biomaterials targeting periodontal regeneration, International Journal of Biological Macromolecules 165 (2020) 2900-2908.
[85] J.-S. Liu, Y.-X. Zeng, S.-Y. Bi, J.-W. Zhou, R. Cheng, J. Li, A.-Q. Jia, Characterization and chemical modification of PLN-1, an exopolysaccharide from *Phomopsis liquidambari* NJUSTb1, Carbohydr. Polym. 253 (2021) 117197.
[86] J. Wang, T. Wu, X. Fang, W. Min, Z. Yang, Characterization and immunomodulatory activity of an exopolysaccharide produced by *Lactobacillus plantarum* JLK0142 isolated from fermented dairy tofu, International journal of biological macromolecules 115 (2018) 985-993.
[87] X. You, L. Yang, X. Zhao, K. Ma, X. Chen, C. Zhang, G. Wang, M. Dong, X. Rui, Q. Zhang, Isolation, purification, characterization and immunostimulatory activity of an exopolysaccharide produced by *Lactobacillus pentosus* LZ-R-17 isolated from Tibetan kefir, International journal of biological macromolecules 158 (2020) 408-419.
[88] I. Uhliariková, M. Šutovská, J. Barboríková, M. Molitorisová, H.J. Kim, Y.I. Park, M. Matulová, J. Lukavský, Z. Hromadková, P. Capek, Structural characteristics and biological effects of exopolysaccharide produced by cyanobacterium *Nostoc* sp, International Journal of Biological Macromolecules 160 (2020) 364-371.
[89] G.S. Nyanhongo, C. Sygmund, R. Ludwig, E.N. Prasetyo, G.M. Guebitz, An antioxidant regenerating system for continuous quenching of free radicals in chronic wounds, Eur. J. Pharm. Biopharm. 83(3) (2013) 396-404.
[90] K. Senni, F. Gueniche, M. Yousfi, F. Fioretti, G.-J. Godeau, S. Colliec-Jouault, J. Ratiskol, C. Sinquin, G. Raguenes, A. Courtois, Sulfated depolymerized derivatives of expolysaccharides (EPS) from mesophilic marine bacteria, method for preparing the same, and uses thereof in tissue regeneration, Google Patents, 2013.
[91] K. Senni, J. Pereira, F. Gueniche, C. Delbarre-Ladrat, C. Sinquin, J. Ratiskol, G. Godeau, A.M. Fischer, D. Helley, S. Colliec-Jouault, Marine polysaccharides: A source of bioactive molecules for cell therapy and tissue engineering, Mar. Drugs 9(9) (2011) 1664-1681.
[92] N.S. Gandhi, R.L. Mancera, The structure of glycosaminoglycans and their interactions with proteins, Chemical Biology and Drug Design 72(6) (2008) 455-482.
[93] P. Priyanka, A. Arun, P. Ashwini, P. Rekha, Functional and cell proliferative properties of an exopolysaccharide produced by *Nitratireductor* sp. PRIM-31, International journal of biological macromolecules 85 (2016) 400-404.
[94] S. Liu, X. Liu, Y. Ren, P. Wang, Y. Pu, R. Yang, X. Wang, X. Tan, Z. Ye, V. Maurizot, Mussel-inspired dual-cross-linking hyaluronic acid/ε-polylysine hydrogel with self-healing and antibacterial properties for wound healing, ACS Applied Materials & Interfaces 12(25) (2020) 27876-27888.
[95] W. Mubarok, Y. Qu, S. Sakai, Influence of Hydrogen Peroxide-Mediated Cross-Linking and Degradation on Cell-Adhesive Gelatin Hydrogels, ACS Applied Bio Materials 4(5) (2021) 4184-4190.

Captions to illustrations

Fig. 1. a) Schematic illustration of EPS extraction and purification from *Cryptococcus laurentii* 70766. **b)** FT-IR spectra of the EPS produced by *C. laurentii* 70766 and sodium alginate.

Fig. 2. a) Schematic figure showing the conjugation reaction of tyramine HCl with **a)** sodium alginate and **b)** EPS (containing the acidic glucuronoxylomannan (GXM) as the main component (about 87%) [24]); (**c**) UV-vis spectra of tyramine, modified EPS (EPS-ty) and EPS, and (**c**) tyramine, modified alginate (Alg-ty) and alginate.

Fig. 3. **a)** The microporous structure of EPS-Ty and Alg-Ty hydrogels. **b)** Swelling ratio% behavior of the hydrogels after 24 h of soaking in PBS buffer. **c)** Degradation profiles of EPS-Ty and Alg-Ty hydrogels in PBS at 37℃. **d)** dynamic viscosity curve of Alg-Ty and EPS-Ty hydrogel. e) The images from EPS-Ty and Alg-Ty hydrogels before and after swelling.

Fig. 4. a) RLU-RealTime-Glo™ cell viability assay of the EPS from *Cryptococcus laurentii 70766* on human fibroblast cell (ATCC: CCL-186) line after 24 h and 30 h of incubation. **b)** RLU-RealTime-Glo™ cell viability assay of the EPS from *C. laurentii 70766* on human macrophage cell line (U937) after 24 h and 30 h of incubation. **c)** Cell viability of 3T3 L cells treated by control (cell culture media), Alg-Ty, and EPS-Ty hydrogels after 24, and 72 h. **d)** Fluorescence microscopy images of live/dead 3T3 L cells seeded on Alg-Ty, EPS-Ty hydrogels, and control (tissue culture plate) after three days. Fluorescent microscopic images of cell-laden Alg-Ty and EPS-Ty hydrogels stained via Hoescht and ethidium homodimer (dead cells) after 1 **(e)** and 3 days **(f)**. Each value is expressed as mean ± SEM (n = 3). $^{a\text{-}d}$ bars that do not share a letter are significantly different at $p < 0.05$.

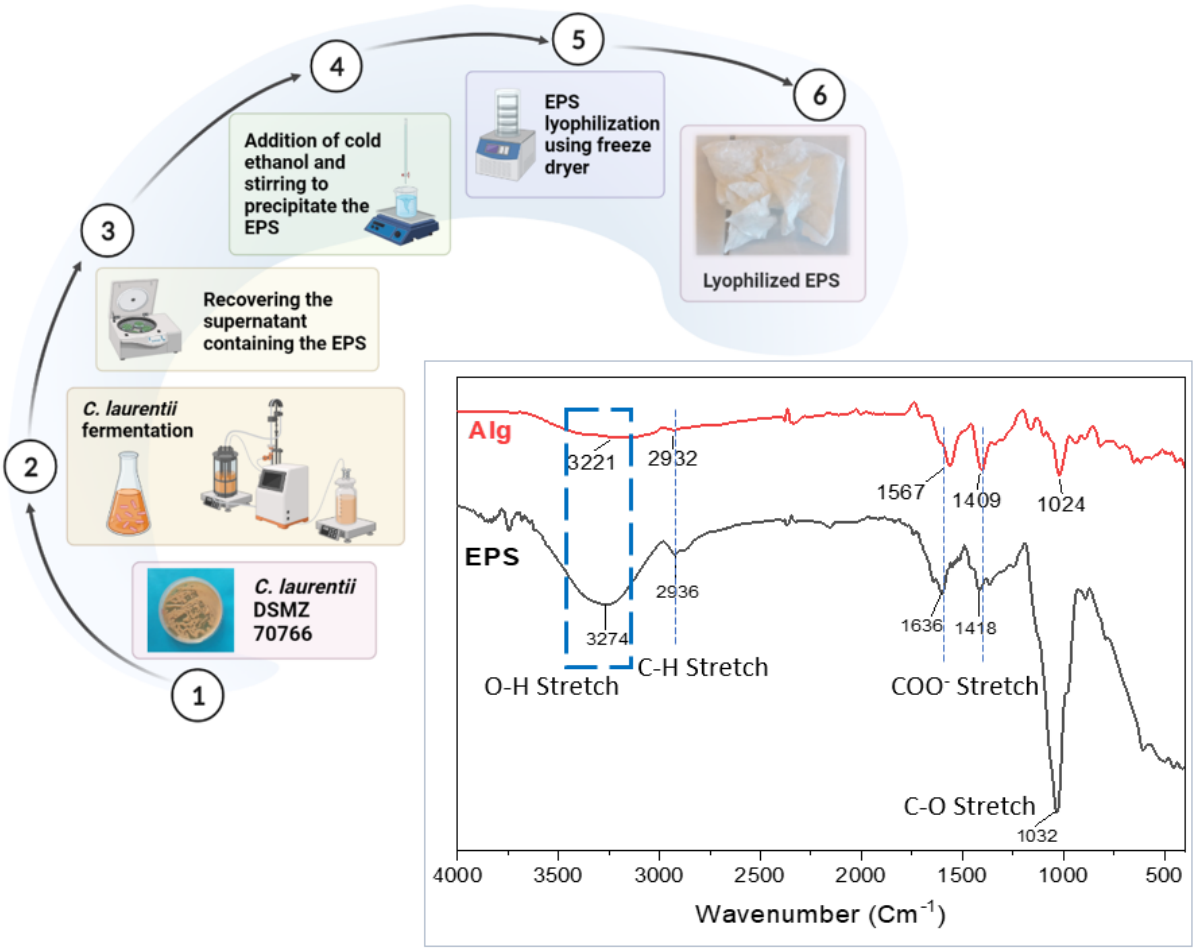

International Journal of Biological Macromolecules, Hamidi et al. Fig. 1

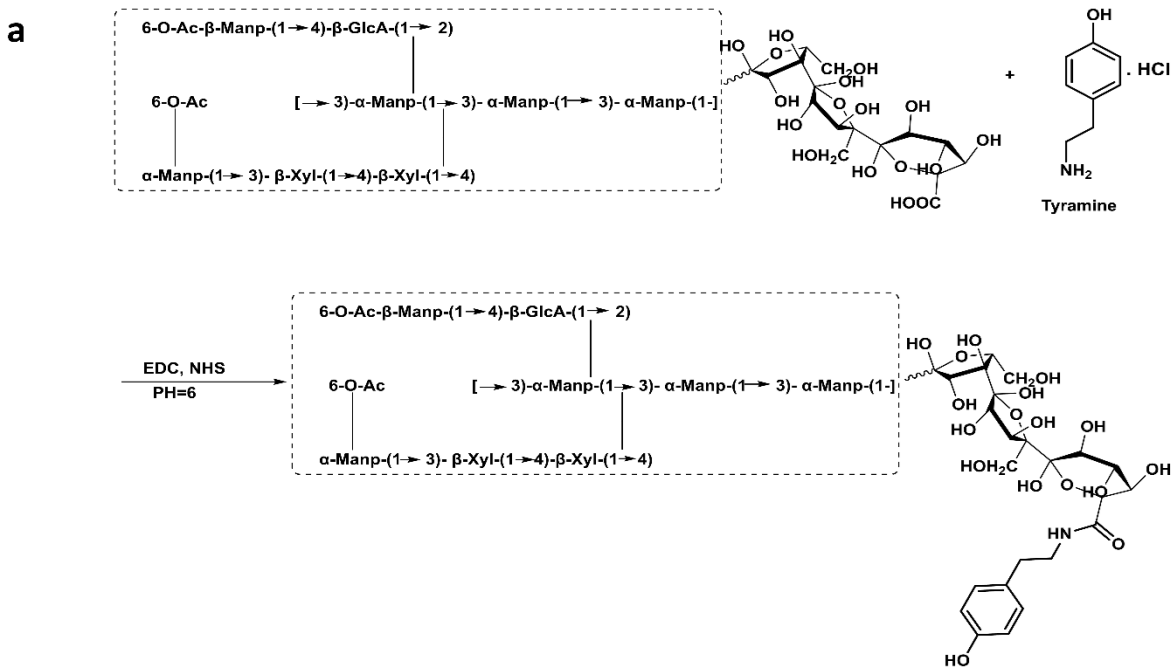

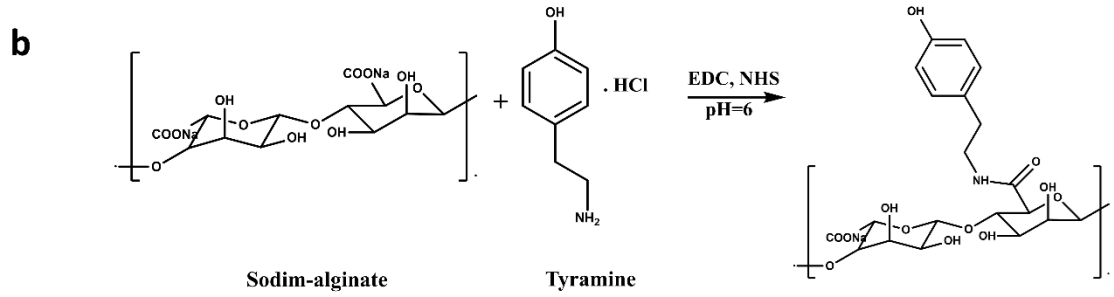

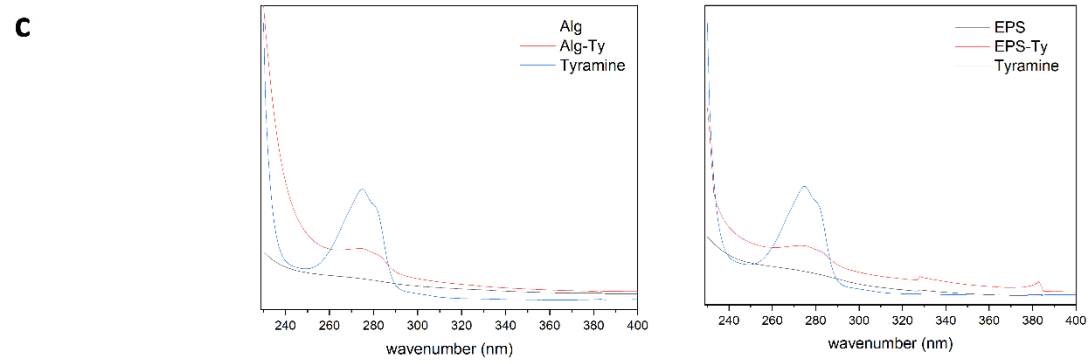

International Journal of Biological Macromolecules, Hamidi et al. Fig. 2

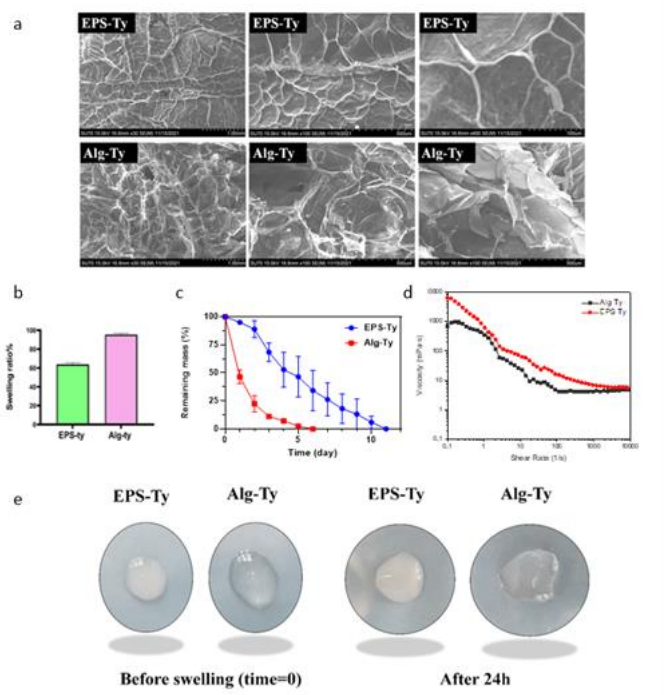

International Journal of Biological Macromolecules, Hamidi et al. Fig. 3

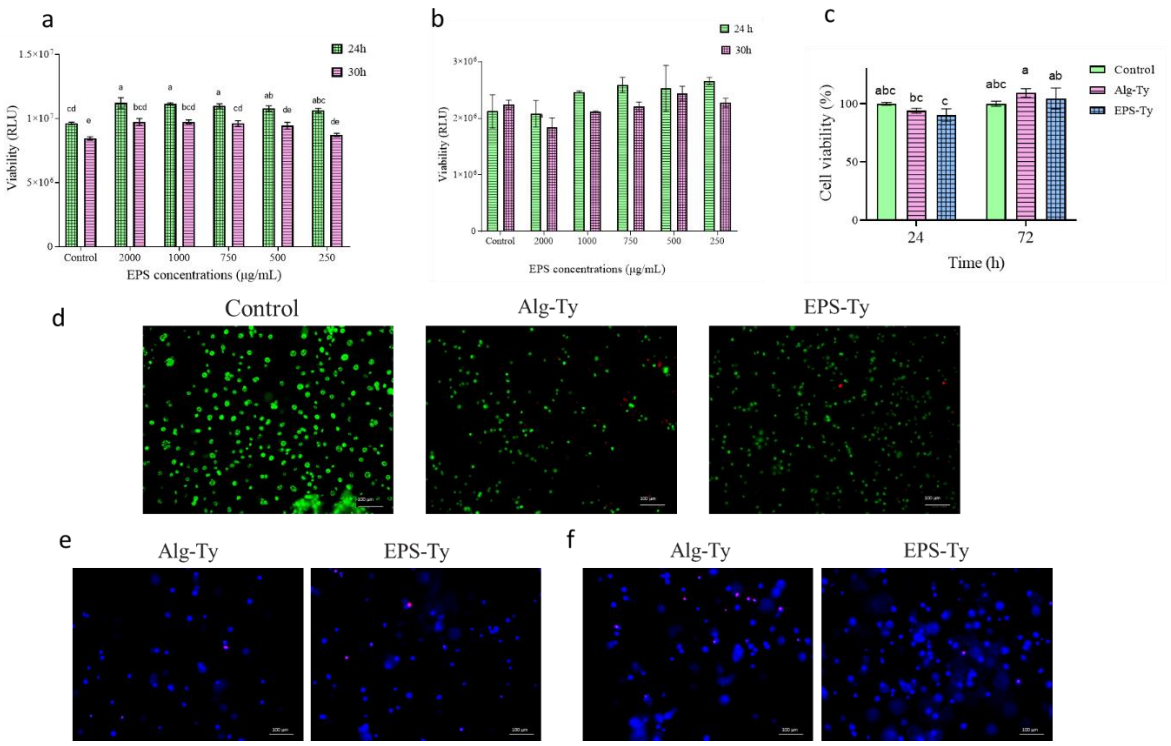

International Journal of Biological Macromolecules, Hamidi et al. Fig. 4